Journal of Molecular Spectroscopy **203,** 28–36 (2000)
doi:10.1006/jmsp.2000.8167, available online at http://www.idealibrary.com on IDEAL®

The $5V_{OH}$ Overtone Transition of HDO

Elena Bertseva, Olga Naumenko,[1] and Alain Campargue[2]

Laboratoire de Spectrométrie Physique (associated with CNRS UMR C5588), Université Joseph Fourier de Grenoble, B.P. 87, 38402 Saint-Martin-d'Hères Cedex, France

Received March 6, 2000; in revised form May 18, 2000

The absorption spectrum of HDO has been recorded by intracavity laser absorption spectroscopy in the 16 540–17 055 cm^{-1} spectral region corresponding to the $5\nu_3$ band centered at 16 920 cm^{-1}. The (0 0 5) vibrational state is found to be mostly isolated from the nearby rovibrational states. The corresponding rovibrational transitions were analyzed and fitted in the frame of the effective rotational Hamiltonian model in Pade–Borel approximants form. The spectroscopic parameters retrieved from the fitting reproduce 100 of the 109 determined energy levels with the root-mean-square deviation of 0.0072 cm^{-1}, close to the experimental accuracy. From the integrated relative intensities of *a*- and *b*-type transitions, the angle between the transition moment and the OH bond is estimated to be 46.4°. This value is consistent with an increasing tilt of the transition dipole moment, away from the OH bond, when the OH stretching is excited. The evolution of the orientation of the transition dipole moment versus the vibrational excitation is then compared for the OH and OD overtone bands.

1. INTRODUCTION

In this work, we continue our systematic exploration of the HDO absorption spectrum in the visible range, recorded by intracavity laser absorption spectroscopy (ICLAS). Our previous reports have concerned the $4\nu_3$ (*1*), $\nu_2 + 4\nu_3$ (*2*), and the $\nu_1 + 3\nu_3$ and $2\nu_2 + 3\nu_3$ bands (*3*). We presently report the spectroscopic analysis of the 16 540–17 055 cm^{-1} spectral region dominated by the $5\nu_3$ band. Note that we do not follow the recommendations of IUPAC and use the traditional labeling of the stretching vibration with ν_1 and ν_3 standing for the OD and OH stretching, respectively.

Contrary to what is indicated in the recent paper of Fair *et al.* (*4*), the $5\nu_3$ band was previously studied by optoacoustic spectroscopy in 1992 (*5*). The (0 0 5) vibrational state was found to be unperturbed by the other rovibrational states. As discussed in Ref. (*1*), the sequences of the (0 0 ν_3) and (ν_1 0 0) vibrational states are isolated, at least up $\nu_3 = 5$ (*5*) and $\nu_1 = 6$ (*2*), respectively. This feature is, partly, a consequence of the detuning between the ω_1 and ω_3 harmonic frequencies resulting from the deuteration of one bond. The highly excited OH and OD stretching states are then localized states of particular interest for studies related to the state-to-state photodissociation dynamics (see Refs. (*4, 6–7*) and references therein). The $5\nu_3$ band is the highest OH overtone transition of the HDO molecule analyzed so far. The knowledge of its energy pattern is a prerequisite for a detailed study of the vibrationally mediated OH bond cleavage. In particular, Brouard *et al.* (*7*) used the (0 0 4) and (0 0 5) states as intermediate excited states in a two-step photodissociation process of HDO and published recently a rough analysis of the corresponding energy levels. In contrast, the forthcoming analysis based on our ICLAS data will confirm and extend significantly the data set of rotational levels previously published in Ref. (*5*). It will allow us to discuss to what extent the (0 0 5) is decoupled from the other vibrational states. Following the approach developed in Ref. (*4*), we will, then, quantitatively analyze the vibrational dependence of the transition dipole-moment vector versus the stretching excitation on the basis of the relative intensity of *a*- and *b*-type transitions.

2. EXPERIMENTAL DETAILS

The ICLAS spectrometer used for the present recording is based on a dye laser cavity in a linear configuration. The technical details and the procedure used for the wavenumber calibration are found in our previous papers (*1–3*) and in the reviews of Refs. (*8–9*). A Rhodamine 6G dye solution was used to record the spectrum between 16 540 and 17 055 cm^{-1}. The intracavity sample cell was filled with a 1:1 mixture of H_2O and D_2O at a pressure of 13 Torr (94 hPa). The spectra below and above 16 600 cm^{-1} were obtained with generation times of 130 and 80 μs, respectively, corresponding to equivalent absorption path lengths of 19.5 and 12 km, respectively. The wavenumber calibration uses two reference lines for each 15 cm^{-1} wide piece of spectrum. The $5V_{OH}$ absorption lines of H_2O (*10*) appearing superimposed on the HDO spectrum were used as references. However, in the region below 16 600 cm^{-1}, where H_2O absorption lines are absent or too sparse, the wavenumber calibration was achieved by simultaneous recording of the iodine absorption spectrum (*11*). We estimate our wavenumber calibration to be accurate to within 0.01 cm^{-1}, as will be confirmed by the uncertainty of the energy levels

[1] On leave from the Institute of Atmospheric Optics, Russian Academy of Sciences, Tomsk, 634055, Russia.

[2] E-mail: Alain.Campargue@ujf-grenoble.fr.

0022-2852/00 $35.00

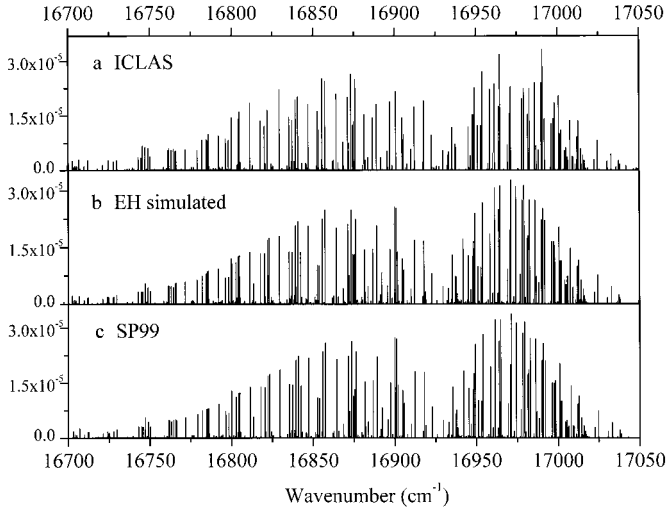

FIG. 1. Comparison of the overview of the $5\nu_3$ band of HDO. (a) Stick spectrum retrieved from our ICLAS data. The absolute intensities were obtained by normalization of the experimental intensities to the total absolute band intensity predicted in Ref. (*12*). Note that a few lines blended with H_2O lines (*10*) observed in (b) and (c) are absent. Note that significant deviations between (a) and both (b) and (c) are observed for the line intensities near 16 975 cm^{-1}. (b) Synthetic spectrum obtained from the effective Hamiltonian (EH) approach. (c) Calculated spectrum predicted by the new *ab initio* calculations of Ref. (*12*).

obtained in the forthcoming rotational analysis. Figure 1 shows the overview of the stick spectrum of HDO retrieved from the ICLAS spectra.

3. RESULTS

A. Energy Levels

We used the parameters derived in Ref. (*5*) as initial rotational and centrifugal distortion constants. Approximate dipole-moment parameters for the *a*- and *b*-type transitions were derived from the fitting to several tens of well-resolved isolated lines providing reasonable intensity predictions for extra line identifications. It was then possible to assign even weak single lines relying on accurate line position and intensity predictions. Finally, 306 transitions (including multiplets) corresponding to 272 lines listed in Table 1 could be rotationally assigned between 16 540 and 17 055 cm^{-1} leaving 10 (4%) weak lines unassigned. Note that about 30 weak lines observed below 16 683 cm^{-1} and belonging partly to the $2\nu_2 + 4\nu_3$ and $\nu_1 + 4\nu_3$ bands are excluded from Table 1 and will be published in a forthcoming contribution. Overall, 109 energy levels, listed in Table 2, were derived by adding the experimental ground state energy levels (*13*) to the observed transitions. The average experimental uncertainty of the levels when observed through several transitions is 0.004 cm^{-1}. Compared to Ref. (*5*), 28 levels were newly observed and five energy levels are corrected by a shift between -0.07 and -0.2 cm^{-1} (see Table 2). Similar to our previous studies (*1–3*), we used the effective Hamiltonian (EH) in the Pade–Borel approximants form to reproduce the energy levels. Using 10 varied parameters listed in Table 3, 100 levels could be fitted, yielding an rms deviation of 0.0072 cm^{-1} close to the experimental accuracy. A very good agreement is observed between our parameter values and those retrieved in the previous analysis (*5*) which, however, used 14 varied parameters to reproduce 86 levels with an rms deviation (0.006 cm^{-1}) similar to ours. Similar to Ref. (*5*), the Δ_{jk} parameter value was found to be very small and poorly determined by the fit. It was then constrained to zero in agreement with the decrease of its value observed between the (0 0 1) and (0 0 4) states (8.1×10^{-4} cm^{-1}) (*14*) and 3.0×10^{-4} (*1*), respectively).

Among the five additional energy levels reported in Ref. (*5*), the [9 7 3] and [9 7 2] levels, which were derived from weak transitions blended with the much stronger [7 1 7]–[7 1 6] line at 16 824.607 cm^{-1}, seem to be incorrect, while the other three levels ([9 4 6], [10 4 7], and [10 6 4]) are confirmed within 0.015 cm^{-1} by our EH calculations. Note that the [9 4 6] level is given in Ref. (*5*) with a misprint; in fact, its value should be 17 781.474 cm^{-1} instead of 17 781.437 cm^{-1}. As in our previous studies (*1–3*), we compare the experimental results with the recent high-quality *ab initio* calculations by Partridge and Schwenke (*15*) as well as with their new version (*12*) which uses an improved dipole-moment surface. The difference between the experimental energy levels and the predictions of Ref. (*12*) are given in the last column of Table 2. The predicted values are higher by about 0.3 cm^{-1} with a maximum deviation of 0.57 cm^{-1}. As previously evidenced for other vibrational states (*1–3*) for high J values, similar deviations are observed for levels with the same K_c value. Among the nine experimental levels excluded from the energy fitting, the [7 5 2] and [11 1 11] levels are probably distorted as derived from unresolved doublet lines. The other seven energy levels deviate from their predicted values by as much as 0.16 cm^{-1}, revealing the occurrence of interaction with dark states. However, except for a couple of levels, namely [9 2 8] and [10 0 10], we could not evidence the interaction scheme responsible of these perturbations. On the basis of the predictions of Ref. (*12*), the (0 4 3), (1 0 4), (1 5 2), and (3 4 1) vibrational states (vibrational assignments of Ref. (*12*)) are possible perturbers of the (0 0 5) state. Intensities ranging between 2.0×10^{-7} and 2.0×10^{-6} cm^{-2}/atm are predicted for some transitions involving these perturbers but only one extra line, namely the [9 6 4]–[8 2 7] transition of the $\nu_1 + 4\nu_3$ band at 17 005.352 cm^{-1}, could be detected and rotationally assigned in our spectra (see Fig. 2). It borrows its intensity from the strong [9 2 8]–[8 2 7] transition of the $5\nu_3$ band at 17 004.182 cm^{-1}. This intensity transfer seems to be confirmed by the value of the EH unperturbed intensity (6.4×10^{-6} cm^{-2}/atm) of the [9 2 8]–[8 2 7] transition of the $5\nu_3$, calculated larger than both the experimental (5.2×10^{-6} cm^{-2}/atm) and predicted (*12*) (4.5×10^{-6} cm^{-2}/atm) values (see next section for a description of the procedure used to determine the experimental and calculated intensities). If the

TABLE 1

Wavenumber, Intensities, and Rovibrational Assignments of the Transitions of $5\nu_3$ Band of HDO between 16 540 and 17 055 cm^{-1}

Observed Wavenumber (cm^{-1})	Intensity (cm^{-2}/atm) Obs.	Calc.	Ref.(*12*)	Upper $J\ K_a\ K_C$	Lower $J\ K_a\ K_C$
B 16542.994	4.0E-07	1.2E-07	1.2E-07	5 5 1	6 6 0
B 16542.994	4.0E-07	1.2E-07	1.2E-07	5 5 0	6 6 1
16587.750	4.0E-07	9.7E-08	9.1E-08	9 6 4	10 6 5
16587.750	4.0E-07	9.7E-08	9.1E-08	9 6 3	10 6 4
16595.272	4.0E-07	1.5E-07	1.4E-07	6 4 2	7 5 3
16605.512	8.0E-07	1.6E-07	1.5E-07	8 6 3	9 6 4
16605.512	8.0E-07	1.6E-07	1.5E-07	8 6 2	9 6 3
16623.110	2.7E-07	2.1E-07	2.1E-07	7 6 2	8 6 3
16623.110	2.7E-07	2.1E-07	2.1E-07	7 6 1	8 6 2
16628.655	9.3E-07	3.1E-07	2.8E-07	4 4 0	5 5 1
16628.655	9.3E-07	3.1E-07	2.8E-07	4 4 1	5 5 0
16635.042	2.7E-07	1.5E-07	1.3E-07	7 3 5	8 4 4
16640.525	8.0E-07	2.0E-07	2.1E-07	6 6 1	7 6 2
16640.525	8.0E-07	2.0E-07	2.1E-07	6 6 0	7 6 1
16654.438	2.5E-07	2.4E-07	2.1E-07	6 3 4	7 4 3
16657.350	3.3E-07	2.1E-07	1.9E-07	12 1 11	13 1 12
16660.768	3.7E-07	2.4E-07	2.0E-07	11 3 9	12 3 10
16663.599	4.0E-07	1.3E-07	1.2E-07	7 2 6	8 3 5
16671.671	2.1E-06	6.7E-07	6.7E-07	7 5 3	8 5 4
16671.671	2.1E-06	6.7E-07	6.7E-07	7 5 2	8 5 3
16672.499	2.9E-07	3.5E-07	3.1E-07	5 3 3	6 4 2
16674.623	3.3E-07	3.4E-07	3.0E-07	5 3 2	6 4 3
16678.632	6.7E-07	5.7E-07	5.2E-07	9 4 5	10 4 6
16679.891	1.1E-06	7.5E-08	5.3E-08	11 1 10	12 2 11
16679.891	1.1E-06	4.4E-07	3.9E-07	12 0 12	13 0 13
16679.891	1.1E-06	4.4E-07	3.9E-07	12 1 12	13 1 13
16680.210	5.3E-07	4.5E-07	3.8E-07	11 2 10	12 2 11
16682.816	4.0E-07	5.3E-07	4.5E-07	10 3 8	11 3 9
16687.918	6.7E-07	3.3E-07	3.0E-07	8 7 2	8 7 1
16687.918	6.7E-07	3.3E-07	3.0E-07	8 7 1	8 7 2
16689.242	2.1E-06	8.4E-07	8.6E-07	6 5 2	7 5 3
16689.242	2.1E-06	8.4E-07	8.6E-07	6 5 1	7 5 2
B 16689.723	6.7E-07	4.8E-07	3.5E-07	4 3 2	5 4 1
16689.856	2.0E-06	6.3E-07	6.1E-07	7 7 0	7 7 1
16689.856	2.0E-06	6.3E-07	6.1E-07	7 7 1	7 7 0
B 16690.304	1.2E-06	4.6E-07	3.1E-07	10 3 7	11 3 8
B 16690.304	1.2E-06	4.7E-07	4.1E-07	4 3 1	5 4 2
16697.256	6.7E-07	6.1E-07	5.3E-07	10 2 8	11 2 9
16699.318	1.2E-06				
16699.484	1.3E-06				
16702.542	2.5E-06	9.2E-07	9.0E-07	11 0 11	12 0 12
16702.542	2.5E-06	9.2E-07	9.0E-07	11 1 11	12 1 12
16702.889	8.0E-07	9.3E-07	7.9E-07	10 2 9	11 2 10
16703.822	8.0E-07	1.0E-06	9.4E-07	9 3 7	10 3 8
16704.848	8.0E-07	9.4E-07	8.0E-07	10 1 9	11 1 10
16706.621	2.8E-06	7.4E-07	7.8E-07	5 5 1	6 5 2
16706.621	2.8E-06	7.4E-07	7.8E-07	5 5 0	6 5 1
16706.621	2.8E-06	6.0E-07	5.1E-07	3 3 0	4 4 1
16709.674	1.1E-06	9.8E-07	9.0E-07	9 3 6	10 3 7
16711.840	2.7E-06	1.6E-06	1.6E-06	7 4 4	8 4 5
16717.849	4.0E-07	4.0E-07	3.4E-07	5 2 4	6 3 3
16721.052	1.3E-06	1.3E-06	1.2E-06	9 2 7	10 2 8
16724.356	1.6E-06	1.8E-06	1.4E-06	10 1 10	11 1 11
16724.558	2.7E-06	1.8E-06	1.3E-06	9 2 8	10 2 9
16727.736	2.3E-06	1.8E-06	1.6E-06	9 1 8	10 1 9
16729.614	2.7E-06	2.3E-06	2.3E-06	6 4 3	7 4 4
16729.679	2.7E-06	2.3E-06	2.3E-06	6 4 2	7 4 3
16734.773	2.1E-07	6.6E-08	7.7E-08	9 3 7	10 2 8
16736.026	2.7E-07	4.4E-07	3.9E-07	5 2 3	6 3 4
16739.349	6.0E-07	5.7E-07	4.8E-07	4 2 3	5 3 2
16742.838	3.5E-06	3.2E-06	3.1E-06	7 3 5	8 3 6
16742.916	2.8E-06	2.6E-06	2.4E-06	8 2 6	9 2 7
16744.720	3.3E-06	3.2E-06	3.1E-06	7 3 4	8 3 5
16744.927	1.6E-06	6.2E-07	5.6E-07	8 6 3	8 6 2
16744.927	1.6E-06	6.2E-07	5.6E-07	8 6 2	8 6 3
16745.479	6.5E-06	3.2E-06	2.9E-06	9 1 9	10 1 10
16746.979	2.9E-06	1.2E-06	1.1E-06	7 6 2	7 6 1
16746.979	2.9E-06	1.2E-06	1.1E-06	7 6 1	7 6 2
16747.116	6.1E-06	2.7E-06	2.8E-06	5 4 1	6 4 2
16747.116	6.1E-06	2.7E-06	2.8E-06	5 4 2	6 4 3
16748.013	4.0E-07	5.8E-07	5.0E-07	4 2 2	5 3 3
B 16748.868	5.8E-06	2.2E-06	2.2E-06	6 6 0	6 6 1
B 16748.868	5.8E-06	2.2E-06	2.2E-06	6 6 1	6 6 0
16750.119	3.6E-06	3.4E-06	3.1E-06	8 1 7	9 1 8
16752.927	2.7E-07	3.4E-07	3.5E-07	8 2 7	9 1 8
16758.438	8.0E-07	7.3E-07	6.0E-07	3 2 2	4 3 1
16760.221	5.3E-07	5.3E-07	5.2E-07	7 1 6	8 2 7
16760.983	2.7E-07	2.9E-07	2.3E-07	4 1 4	5 2 3
16761.158	5.3E-06	4.7E-06	4.7E-06	6 3 4	7 3 5
16761.542	5.3E-07	7.3E-07	6.0E-07	3 2 1	4 3 2
16761.694	5.9E-06	4.8E-06	4.8E-06	6 3 3	7 3 4
16763.044	5.3E-06	4.6E-06	4.5E-06	7 2 5	8 2 6
16764.359	5.6E-06	2.2E-06	2.4E-06	4 4 1	5 4 2
16764.359	5.6E-06	2.2E-06	2.4E-06	4 4 0	5 4 1
16765.456	5.1E-06	5.3E-06	5.0E-06	7 2 6	8 2 7
16765.785	5.1E-06	5.5E-06	4.7E-06	8 1 8	9 1 9
16766.043	5.1E-06	5.5E-06	4.7E-06	8 0 8	9 0 9
16769.292	3.5E-07	1.2E-07	1.2E-07	4 1 4	4 3 1
16771.434	6.7E-07	2.8E-07	2.2E-07	9 1 8	9 3 7
16771.434	6.7E-07	2.8E-07	2.2E-07	9 0 9	9 2 8
16771.597	5.5E-06	5.8E-06	5.6E-06	7 1 6	8 1 7
16775.474	8.0E-07	6.8E-07	6.4E-07	6 1 5	7 2 6
16776.575	8.0E-07	8.5E-07	6.8E-07	2 2 0	3 3 1
16776.843	5.2E-07	4.5E-07	4.6E-07	7 2 6	8 1 7
16778.932	5.3E-06	6.2E-06	6.4E-06	5 3 3	6 3 4
16781.918	8.0E-06	7.4E-06	7.4E-06	6 2 4	7 2 5
16784.454	8.1E-06	8.0E-06	7.9E-06	6 2 5	7 2 6
16785.077	1.3E-06	1.3E-06	1.3E-06	7 0 7	8 1 8
16785.324	7.9E-06	8.6E-06	8.0E-06	7 1 7	8 1 8
B 16785.762	9.6E-06	8.7E-06	8.0E-06	7 0 7	8 0 8
16786.016	1.2E-06	1.3E-06	1.3E-06	7 1 7	8 0 8
16787.143	2.5E-07	1.6E-07	1.2E-07	10 2 9	10 2 8
16788.782	4.4E-07	7.9E-07	7.2E-07	5 1 4	6 2 5
16789.317	2.0E-07	2.0E-07	1.6E-07	10 5 6	10 5 5
16790.034	4.0E-07	4.6E-07	3.7E-07	3 1 3	4 2 2
16790.533	3.7E-07	4.8E-07	4.2E-07	8 0 8	8 2 7
16791.982	9.2E-06	9.3E-06	9.2E-06	6 1 5	7 1 6
16792.675	5.3E-07	4.5E-07	3.7E-07	9 5 4	9 5 5
16793.261	4.0E-07	5.9E-07	5.4E-07	7 1 6	7 3 5
16794.367	8.0E-07	9.6E-07	8.4E-07	8 5 3	8 5 4
16796.131	8.4E-06	6.9E-06	7.2E-06	4 3 1	5 3 2
16796.324	7.2E-06	6.9E-06	6.2E-06	4 3 2	5 3 3
16796.854	1.6E-07	1.0E-07	1.1E-07	3 1 2	3 3 1
16798.085	8.0E-06	3.6E-06	3.4E-06	6 5 1	6 5 2
16798.085	8.0E-06	3.6E-06	3.4E-06	6 5 2	6 5 1
16799.094	3.3E-07	2.9E-07	3.0E-07	4 1 3	4 3 2
16799.823	1.4E-05	6.3E-06	6.4E-06	5 5 1	5 5 0
16799.823	1.4E-05	6.3E-06	6.4E-06	5 5 0	5 5 1
16800.010	1.2E-05	1.1E-05	1.1E-05	5 2 3	6 2 4
16803.487	1.5E-06	1.6E-06	1.6E-06	6 0 6	7 1 7
16804.055	1.4E-05	1.3E-05	1.2E-05	6 1 6	7 1 7
16804.773	1.6E-05	1.3E-05	1.2E-05	6 0 6	7 0 7
B 16805.333	2.1E-06	1.6E-06	1.5E-06	6 1 6	7 0 7
16807.496	2.3E-07	1.4E-07	1.5E-07	2 0 2	3 2 1
16807.847	6.8E-07	7.6E-07	6.9E-07	7 0 7	7 2 6
16808.973	3.9E-07				
16811.136	1.8E-05	1.4E-05	1.4E-05	5 1 4	6 1 5
16812.493	4.0E-07	3.2E-07	1.9E-07	9 2 8	9 2 7
16812.872	1.3E-06	8.9E-07	7.4E-07	3 1 2	4 2 3
16817.681	1.3E-05	1.3E-05	1.4E-05	4 2 2	5 2 3
16820.122	1.2E-05	1.3E-05	1.4E-05	4 2 3	5 2 4
16820.748	1.7E-06	1.9E-06	1.7E-06	5 0 5	6 1 6
16821.974	1.6E-05	1.7E-05	1.7E-05	5 1 5	6 1 6
16824.274	1.7E-06	1.8E-06	1.7E-06	5 1 5	6 0 6
16824.607	8.9E-07	7.6E-07	6.9E-07	7 1 7	7 1 6
16825.000	4.7E-07	5.4E-07	5.1E-07	5 2 4	6 1 5

Note. The experimental, calculated (EH), and predicted (*12*) intensities are given in cm^{-2}/atm at 296 K and correspond to pure HDO. The total calculated and experimental line intensities are normalized (see text) to the total HDO intensity predicted in Ref. (*12*). T means tentative assignment. The asterisk (*) marks the extra line of the $\nu_1 + 4\nu_3$ band (see text). In the case of unresolved multiplets, the same experimental intensity is given for the different components while the calculated intensities from the EH or from Ref. (*12*) correspond to each component. HDO lines blended with H_2O lines are marked by (B).

TABLE 1—*Continued*

Observed Wavenumber (cm^{-1})	Intensity (cm^{-2}/atm) Obs.	Calc.	Ref.(*12*)	Upper $J\ K_a\ K_C$	Lower $J\ K_a\ K_C$	Observed Wavenumber (cm^{-1})	Intensity (cm^{-2}/atm) Obs.	Calc.	Ref.(*12*)	Upper $J\ K_a\ K_C$	Lower $J\ K_a\ K_C$
16825.309	1.1E-06	8.8E-07	6.9E-07	2 1 1	3 2 2	16904.517	1.4E-05	1.2E-05	1.3E-05	0 0 0	1 0 1
16829.328	2.2E-05	1.8E-05	1.9E-05	4 1 3	5 1 4	16904.632	8.1E-06	7.5E-06	7.5E-06	4 2 2	4 2 3
16831.031	5.3E-07	9.3E-08	9.2E-08	7 1 7	6 3 4	16905.032	2.7E-06	1.4E-06	1.4E-06	7 5 3	6 5 2
16833.948	1.2E-06	1.2E-06	1.0E-06	8 4 5	8 4 4	16905.032	2.7E-06	1.4E-06	1.4E-06	7 5 2	6 5 1
16835.190	1.4E-05	1.4E-05	1.5E-05	3 2 1	4 2 2	16905.436	9.5E-06	8.3E-06	8.7E-06	2 1 2	2 1 1
16835.584	8.8E-07	6.4E-07	5.4E-07	8 2 7	8 2 6	16905.436	9.5E-06	7.2E-07	7.5E-07	4 0 4	3 2 1
16836.633	1.7E-06	2.0E-06	1.7E-06	4 0 4	5 1 5	16906.570	5.5E-07				
16836.802	2.4E-06	2.3E-06	2.1E-06	7 4 4	7 4 3	16907.524	1.6E-06	8.3E-07	8.5E-07	5 0 5	4 2 2
16837.069	1.3E-05	1.4E-05	1.4E-05	3 2 2	4 2 3	16909.926	5.6E-06	3.9E-06	3.8E-06	5 2 3	5 2 4
16838.236	1.3E-06	1.1E-06	9.4E-07	8 4 4	8 4 5	16912.043	1.7E-05	1.7E-05	1.8E-05	1 1 1	1 1 0
16838.345	2.4E-06	2.3E-06	2.1E-06	7 4 3	7 4 4	16917.171	2.1E-06	2.0E-06	1.8E-06	6 2 4	6 2 5
16838.965	4.7E-06	4.4E-06	4.2E-06	6 4 3	6 4 2	16917.756	1.9E-05	1.7E-05	1.8E-05	1 1 0	1 1 1
16839.104	1.9E-05	2.1E-05	2.1E-05	4 1 4	5 1 5	16922.559	9.4E-06	8.1E-06	8.5E-06	2 1 1	2 1 2
16839.406	4.8E-06	4.4E-06	4.2E-06	6 4 2	6 4 3	16922.740	8.6E-07				
16839.809	3.9E-07	4.8E-07	3.8E-07	9 4 5	9 4 6	16925.701	1.1E-06	9.9E-07	8.6E-07	7 2 5	7 2 6
16840.217	2.7E-07	4.5E-07	3.6E-07	9 3 7	9 3 6	16929.520	5.3E-06	4.6E-06	4.8E-06	3 1 2	3 1 3
16840.553	2.0E-05	2.2E-05	2.2E-05	4 0 4	5 0 5	16932.059	6.7E-07	9.4E-07	6.4E-07	1 1 0	1 0 1
16840.754	9.0E-06	8.0E-06	7.9E-06	5 4 2	5 4 1	16932.226	1.3E-06	8.5E-07	8.0E-07	9 5 5	8 5 4
16840.828	8.0E-06	8.0E-06	7.9E-06	5 4 1	5 4 2	16932.688	4.1E-06	4.2E-06	4.3E-06	6 4 3	5 4 2
16843.020	1.9E-06	1.8E-06	1.6E-06	4 1 4	5 0 5	16932.926	7.3E-07	8.4E-07	8.0E-07	9 5 4	8 5 3
16845.458	1.9E-06	1.4E-06	1.4E-06	4 0 4	4 2 3	B 16933.050	4.9E-06	4.2E-06	4.3E-06	6 4 2	5 4 1
16845.997	1.5E-06	1.2E-06	1.1E-06	6 1 6	6 1 5	16934.789	2.9E-07	2.5E-07	1.3E-07	2 0 2	1 1 1
16846.927	1.8E-05	2.1E-05	2.2E-05	3 1 2	4 1 3	16935.082	1.1E-05	1.3E-05	1.4E-05	1 0 1	0 0 0
B 16847.924	2.7E-07	3.5E-07	1.9E-07	4 1 4	4 2 3	16935.401	3.6E-07				
16852.005	1.1E-06	1.0E-06	1.1E-06	3 0 3	3 2 2	16936.969	7.0E-06	7.3E-06	6.6E-06	4 3 2	3 3 1
16852.545	1.6E-05	1.0E-05	1.1E-05	2 2 0	3 2 1	16937.483	6.1E-06	7.2E-06	7.7E-06	4 3 1	3 3 0
16853.340	6.7E-07	1.0E-06	8.5E-07	8 3 6	8 3 5	16939.561	2.7E-07	7.2E-07	4.7E-07	6 2 4	6 1 5
16853.603	1.1E-05	1.0E-05	1.1E-05	2 2 1	3 2 2	16943.636	2.7E-07	2.4E-07	1.9E-07	6 4 2	6 3 3
16855.301	2.8E-06	3.3E-07	3.5E-07	7 6 2	6 6 1	16945.190	1.2E-05	1.3E-05	1.4E-05	3 2 2	2 2 1
16855.301	2.8E-06	3.3E-07	3.5E-07	7 6 1	6 6 0	16945.422	2.1E-07	2.3E-07	1.9E-07	6 4 3	6 3 4
16855.301	2.8E-06	1.3E-06	1.1E-06	7 2 6	7 2 5	16945.608	7.3E-07	5.2E-07	4.8E-07	10 5 6	9 5 5
16855.494	2.4E-05	2.3E-05	2.4E-05	3 1 3	4 1 4	16946.524	3.9E-06	3.8E-06	3.8E-06	7 4 4	6 4 3
16856.496	4.0E-07	3.8E-07	2.3E-07	3 1 3	3 2 2	B 16946.669	7.3E-07	2.5E-07	2.0E-07	5 4 1	5 3 2
16857.232	2.4E-05	2.5E-05	2.6E-05	3 0 3	4 0 4	16947.755	1.5E-05	1.2E-05	1.3E-05	3 2 1	2 2 0
B 16861.729	2.4E-06	1.6E-06	1.3E-06	3 1 3	4 0 4	16948.198	1.5E-05	1.7E-05	1.8E-05	2 1 1	1 1 0
16862.488	2.7E-06	2.1E-06	1.9E-06	7 3 5	7 3 4	16948.704	2.7E-07	5.2E-07	3.9E-07	4 3 1	4 2 2
16862.720	3.2E-07	3.1E-07	2.0E-07	2 1 2	2 2 1	16949.052	2.2E-05	2.4E-05	2.6E-05	2 0 2	1 0 1
16864.226	2.0E-05	2.0E-05	2.1E-05	2 1 1	3 1 2	16950.961	1.2E-05	9.9E-06	1.0E-05	5 3 3	4 3 2
16865.350	2.0E-06	1.9E-06	1.9E-06	5 1 5	5 1 4	16952.844	1.2E-05	9.7E-06	1.0E-05	5 3 2	4 3 1
B 16868.393	7.5E-06	4.1E-06	3.9E-06	6 3 4	6 3 3	16953.745	2.6E-05	2.7E-05	2.8E-05	3 1 3	2 1 2
16868.790	1.1E-06	3.8E-07	3.8E-07	8 6 3	7 6 2	16956.545	2.7E-07	2.7E-08	1.5E-08	11 2 9	11 1 10
16868.790	1.1E-06	3.8E-07	3.8E-07	8 6 2	7 6 1	16956.545	2.7E-07	9.6E-08	6.5E-08	9 3 7	9 2 8
16869.673	2.0E-07	5.1E-07	2.9E-07	5 1 4	5 2 3	16957.287	1.7E-06	1.0E-06	9.4E-07	6 1 5	6 1 6
16871.229	1.9E-05	2.1E-05	2.2E-05	2 1 2	3 1 3	16958.383	2.2E-05	1.9E-05	1.9E-05	4 2 3	3 2 2
16872.050	7.3E-06	7.5E-06	7.4E-06	5 3 3	5 3 2	16959.578	2.7E-07	4.4E-07	2.9E-07	6 1 5	6 0 6
16873.231	2.6E-05	2.5E-05	2.6E-05	2 0 2	3 0 3	16960.036	4.5E-06	2.9E-06	2.8E-06	8 4 5	7 4 4
16874.311	1.2E-05	1.3E-05	1.1E-05	4 3 2	4 3 1	16961.216	2.3E-05	3.1E-05	3.2E-05	3 0 3	2 0 2
16874.862	1.3E-05	7.2E-06	7.1E-06	5 3 2	5 3 3	16961.650	2.0E-06	4.8E-07	3.3E-07	5 2 4	5 1 5
16875.814	2.4E-05	2.2E-05	2.4E-05	3 3 1	3 3 0	16963.730	1.7E-05	2.5E-05	2.6E-05	3 1 2	2 1 1
16875.909	2.2E-05	2.2E-05	2.3E-05	3 3 0	3 3 1	16964.580	3.1E-05	3.1E-05	3.2E-05	4 1 4	3 1 3
16880.303	1.3E-06	1.1E-06	8.8E-07	2 1 2	3 0 3	16966.984	3.2E-07	2.7E-07	1.7E-07	7 1 6	7 0 7
16881.385	1.5E-05	1.4E-05	1.5E-05	1 1 0	2 1 1	16969.251	6.8E-06	9.2E-06	9.3E-06	6 3 3	5 3 2
16881.987	2.7E-06	3.0E-06	3.0E-06	4 1 4	4 1 3	16970.473	1.5E-05	1.9E-05	2.0E-05	5 2 4	4 2 3
16882.185	4.0E-07	3.0E-07	2.9E-07	9 6 3	8 6 2	16971.168	2.2E-05	3.3E-05	3.4E-05	4 0 4	3 0 3
16882.185	4.0E-07	3.0E-07	2.9E-07	9 6 4	8 6 3	16976.106	2.7E-07	3.1E-07	2.4E-07	8 2 7	8 0 8
16883.512	3.5E-06	4.5E-06	4.4E-06	5 2 4	5 2 3	16978.105	1.9E-05	2.7E-05	2.9E-05	4 1 3	3 1 2
16886.412	1.4E-05	1.5E-05	1.6E-05	1 1 1	2 1 2	16979.208	2.2E-05	3.1E-05	3.2E-05	5 0 5	4 0 4
16887.298	2.7E-07	1.5E-07	1.3E-07	10 2 8	9 4 5	16981.720	1.5E-05	1.8E-05	1.9E-05	5 2 3	4 2 2
16888.900	1.8E-05	2.1E-05	2.2E-05	1 0 1	2 0 2	16982.635	2.2E-05	2.7E-05	2.7E-05	6 1 6	5 1 5
16891.280	3.5E-06	1.2E-06	1.2E-06	6 5 1	5 5 0	16985.987	2.3E-05	2.7E-05	2.7E-05	6 0 6	5 0 5
16891.280	3.5E-06	1.2E-06	1.2E-06	6 5 2	5 5 1	16986.851	6.5E-06	7.2E-06	7.1E-06	7 3 4	6 3 3
16892.523	2.1E-07	1.6E-07	1.3E-07	2 2 1	3 1 2	16988.233	5.4E-06	5.7E-06	5.4E-06	8 3 6	7 3 5
16895.410	5.1E-06	4.9E-06	5.0E-06	3 1 3	3 1 2	16989.925	2.3E-05	2.2E-05	2.1E-05	7 1 7	6 1 6
16897.025	1.8E-05	1.4E-05	1.5E-05	3 2 2	3 2 1	16990.538	1.6E-05	1.4E-05	1.3E-05	7 2 6	6 2 5
16898.131	3.3E-07	3.0E-07	3.2E-07	3 0 3	2 2 0	16990.680	3.2E-05	2.5E-05	2.6E-05	5 1 4	4 1 3
16898.390	1.3E-06	5.0E-07	3.9E-07	1 1 1	2 0 2	16991.966	1.4E-05	2.2E-05	2.1E-05	7 0 7	6 0 6
16898.390	1.3E-06	1.0E-06	6.5E-07	2 0 2	2 1 1	16995.443	6.9E-07	6.2E-07	5.2E-07	11 4 8	10 4 7
16900.672	2.1E-05	2.5E-05	2.7E-05	2 2 0	2 2 1	16996.133	1.2E-05	1.7E-05	1.5E-05	8 1 8	7 1 7
16901.018	3.1E-07	3.3E-07	2.9E-07	9 1 8	8 3 5	16997.311	1.4E-05	1.6E-05	1.5E-05	8 0 8	7 0 7

TABLE 1—*Continued*

Observed Wavenumber (cm^{-1})	Intensity (cm^{-2}/atm) Obs.	Calc.	Ref.(*12*)	Upper $J\ K_a\ K_C$	Lower $J\ K_a\ K_C$	Observed Wavenumber (cm^{-1})	Intensity (cm^{-2}/atm) Obs.	Calc.	Ref.(*12*)	Upper $J\ K_a\ K_C$	Lower $J\ K_a\ K_C$
16998.042	1.8E-05	1.6E-05	1.6E-05	6 2 4	5 2 3	17012.928	2.7E-07	2.8E-07	9.4E-08	4 3 2	3 2 1
16998.222	9.1E-06	9.7E-06	8.8E-06	8 2 7	7 2 6	17014.245	5.7E-06	6.3E-06	5.5E-06	9 1 8	8 1 7
17000.658	2.0E-05	2.0E-05	2.0E-05	6 1 5	5 1 4	T 17014.619	1.5E-06	6.2E-07	3.9E-07	14 1 14	13 1 13
17001.370	9.7E-06	1.1E-05	1.0E-05	9 1 9	8 1 8	T 17014.619	1.5E-06	6.2E-07	3.9E-07	14 0 14	13 0 13
17002.008	1.1E-05	1.1E-05	1.0E-05	9 0 9	8 0 8	17015.584	4.0E-06	3.8E-06	3.3E-06	10 1 9	9 1 8
17004.182	5.2E-06	6.4E-06	4.5E-06	9 2 8	8 2 7	17016.335	2.7E-06	2.2E-06	1.8E-06	11 1 10	10 1 9
17005.000	6.0E-06	5.0E-06	4.8E-06	8 3 5	7 3 4	17016.694	1.2E-06	1.1E-06	9.0E-07	12 1 11	11 1 10
*T17005.352	1.5E-06		1.3E-06	9 6 4	8 2 7	17017.311	4.9E-07	5.3E-07	4.5E-07	11 4 7	10 4 6
17005.692	3.5E-06	7.3E-06	3.0E-06	10 1 10	9 1 9	17018.339	5.9E-07				
17005.848	3.1E-06	2.3E-09	2.9E-06	10 0 10	9 1 9	17022.448	2.8E-06	3.2E-06	2.9E-06	9 3 6	8 3 5
17005.974	1.7E-06	2.2E-06	1.9E-06	10 3 8	9 3 7	17024.444	8.0E-06	7.7E-06	7.3E-06	8 2 6	7 2 5
17006.052	3.5E-06	2.3E-09	3.3E-06	10 1 10	9 0 9	17030.350	2.4E-06	1.6E-06	1.7E-06	4 2 2	3 0 3
17006.209	2.7E-06	7.3E-06	2.4E-06	10 0 10	9 0 9	17030.753	5.7E-07				
17007.655	1.3E-05	1.5E-05	1.4E-05	7 1 6	6 1 5	17032.812	4.3E-06	4.6E-06	4.2E-06	9 2 7	8 2 6
17008.913	3.6E-06	3.9E-06	3.3E-06	10 2 9	9 2 8	T 17035.858	8.8E-07	5.9E-07	3.4E-07	12 2 10	11 2 9
17009.329	3.6E-06	4.4E-06	3.2E-06	11 0 11	10 0 10	17037.300	2.5E-06	2.5E-06	2.1E-06	10 2 8	9 2 7
17010.854	1.6E-06	9.7E-07	1.0E-06	3 2 1	2 0 2	17037.672	1.6E-06	1.8E-06	1.2E-06	10 3 7	9 3 6
17011.756	2.7E-06	2.4E-06	1.9E-06	12 1 12	11 1 11	17038.184	1.6E-06	1.2E-06	1.0E-06	11 2 9	10 2 8
17011.928	8.9E-06	1.0E-05	9.3E-06	8 1 7	7 1 6	17051.156	3.5E-07				
17012.180	2.5E-06	2.2E-06	1.8E-06	11 2 10	10 2 9	17052.703	5.7E-07				
17012.588	1.3E-05	1.2E-05	1.1E-05	7 2 5	6 2 4	17054.065	7.2E-07	3.6E-07	4.0E-07	4 3 1	3 1 2

other predicted (*12*) extra lines are not blended, we conclude that their intensities are predicted to be too strong. In particular, the relatively strong predicted transitions reaching the [4 3 2] (3 4 1) level are not observed in our spectra in agreement with the absence of observed perturbations either in position or in intensity of the corresponding line partners reaching the [4 3 2] (0 0 5) level.

Note that the rough rotational analysis presented recently in Ref. (*7*) gives an erroneous band center shifted at -8.2 cm^{-1} from our value. The $n\nu_3$ (n = 1–5) band origins can be reproduced with an rms of 2.1 cm^{-1} by the standard expression of the energy levels of a single Morse oscillator

$$G(n) = \omega_3(n + 1/2) + x_{33}(n + 1/2)^2, \qquad [1]$$

with $\omega_3 = 3865.60(24)$ cm^{-1} and $x_{33} = -80.323(56)$ cm^{-1}. These values of ω_3 and x_{33} differ significantly from those obtained in Ref. (*4*), indicating the limited predictive ability of this two-parameter model. A much better fit (rms = 0.10 cm^{-1}) can be achieved by adding a third-order term, $y_{333}(n + 1/2)^3$, in the above term value. The corresponding values of the parameters are (in cm^{-1}) $\omega_3 = 3875.057(40)$, $x_{33} = -84.528(18)$, and $y_{333} = 0.4845(23)$.

B. Line Intensities

To give an estimation of the absolute intensities of the observed absorption lines, we normalized our relative experimental intensities on the total predicted (*12*) absolute intensity of the $5\nu_3$ band. After normalization, 65% of all 272 experimental line intensities coincide within 25% with the predicted values. In our data set, only 59 weak lines corresponding to b-type transitions with intensities ranging from 2.0×10^{-7} up to 2.4×10^{-6} cm^{-2}/atm could be identified. Considering that our experimental procedure consisting of retrieving the line intensity from the peak depth is not accurate for weak lines, we used the intensity predictions of Ref. (*12*) to determine the relevant transition moment parameters. Then some of the relevant parameters were constrained to zero in the fitting process of the experimental intensities leading to the results presented in Table 4. Three well-determined parameters are needed to reproduce the 38 b-type experimental intensities. Overall, seven parameters of the transformed dipole-moment operator were obtained by fitting to 210 of 274 experimental intensities. The average deviation is 13% with 63% of the fitted line intensities reproduced within 15%. The ratio of the total intensity of a-type (1.96×10^{-3} cm^{-2}/atm) to b-type (9.7×10^{-5} cm^{-2}/atm) transitions calculated with these parameters is 20, very close to the predicted (*12*) value of 23.7. The intensity ratio of the experimentally observed a- and b-type transitions is 34, probably indicating that a number of b-type transitions were blended or too weak to be measured. Figures 1 and 2 show the good agreement achieved between the experimental, EH synthetic, and *ab initio* (*12*) spectrum for the whole spectrum and an expanded region, respectively.

An interesting case of resonance intensity redistribution is observed for transitions just above 17 005 cm^{-1} reaching the [10 0 10] and [10 1 10] levels (see Fig. 2). According to the predictions of Ref. (*12*), these levels are perturbed by the [10 5 6] level of the (1 0 4) state. This resonance interaction leads to the inversion in the energy order of the [10 0 10] and [10 1 10] levels and originates an intensity transfer from a- to b-type transitions, though only the energy value of the [10 0 10] level appears to deviate significantly from the EH predictions. As discussed above, the $5\nu_3$ band is mainly of a-type. However, in the case of the four transitions involving the the [10 0 10] and [10 1 10] levels, a- and b-type intensities are similar (see Table

TABLE 2
Rotational Energy Levels (cm^{-1}) of the (0 0 5) Vibrational State of HDO

$J\ K_a\ K_c$	E_{obs}	σ	N	obs.-calc.	Δ	$J\ K_a\ K_c$	E_{obs}	σ	N	obs.-calc.	Δ
0 0 0	16920.024		1	0.001	-0.26	7 3 4	17456.515	0.001	3	0.003	-0.23
1 0 1	16935.077	0.004	2	-0.001	-0.27	7 4 4	17520.409	0.005	3	-0.007	-0.20
1 1 1	16944.539	0.001	2	-0.004	-0.27	7 4 3	17521.669		1	-0.005	-0.21
1 1 0	16947.567	0.002	3	-0.002	-0.26	7 5 3	17614.201	0.002	2	0.005	-0.16
2 0 2	16964.560	0.001	3	-0.004	-0.27	7 5 2*	17614.216	0.016	2	-0.031	-0.20
2 1 2	16971.624	0.006	3	0.002	-0.26	7 6 2	17728.110	0.003	2	0.002	-0.12
2 1 1	16980.691	0.005	4	0.001	-0.26	7 6 1	17728.110	0.004	2	0.001	-0.13
2 2 1	17008.987	0.004	2	-0.002	-0.25	7 7 1	17861.388 n		1	0.001	-0.08
2 2 0	17009.602	0.005	3	-0.002	-0.25	7 7 0	17861.388 n		1	0.001	-0.07
3 0 3	17007.392	0.005	4	0.004	-0.27	8 0 8	17400.474	0.004	3	0.005	-0.26
3 1 3	17011.876	0.006	6	0.001	-0.26	8 1 8	17400.577	0.001	2	0.001	-0.26
3 1 2	17029.912	0.002	4	0.003	-0.25	8 1 7	17485.850	0.004	2	0.001	-0.25
3 2 2	17054.114	0.002	3	-0.001	-0.24	8 2 7	17488.661	0.009	3	0.013	-0.23
3 2 1	17057.026	0.002	4	-0.003	-0.25	8 2 6	17544.564 n	0.003	2	0.003	-0.25
3 3 1	17108.865		1	0.003	-0.22	8 3 6	17565.136	0.001	2	0.002	-0.24
3 3 0	17108.941	0.009	2	-0.001	-0.22	8 3 5	17586.962		1	-0.004	-0.23
4 0 4	17062.498	0.001	4	0.001	-0.26	8 4 5	17643.350	0.009	2	0.003	-0.21
4 1 4	17064.969	0.004	7	0.001	-0.26	8 4 4	17646.799		1	-0.003	-0.23
4 1 3	17094.565	0.001	2	0.001	-0.26	8 5 3	17736.899		1	-0.003	-0.18
4 2 3	17113.763	0.006	3	0.002	-0.24	8 6 3	17849.924	0.006	2	-0.009	-0.13
4 2 2	17121.677	0.002	4	-0.001	-0.25	8 6 2	17849.923	0.006	2	-0.016	-0.16
4 3 2	17169.989	0.004	5	-0.004	-0.23	8 7 2	17982.754 n		1	0.001	-0.11
4 3 1	17170.540	0.004	4	0.003	-0.23	8 7 1	17982.754 n		1	0.001	-0.09
4 4 1	17244.612 n	0.011	2	0.003	-0.19	9 0 9	17514.527	0.004	2	-0.005	-0.28
4 4 0	17244.620 n	0.003	2	0.003	-0.21	9 1 9	17514.586	0.009	2	0.009	-0.28
5 0 5	17129.362	0.002	3	-0.004	-0.26	9 1 8*	17612.805 n	0.005	4	-0.058	-0.24
5 1 5	17130.588	0.001	3	-0.003	-0.26	9 2 8*	17614.133 n	0.004	3	-0.134	-0.20
5 1 4	17173.663	0.004	3	0.014	-0.24	9 2 7	17685.901 c	0.001	2	-0.004	-0.27
5 2 4	17187.511	0.004	5	0.003	-0.24	9 3 7	17699.616	0.006	3	0.024	-0.25
5 2 3	17203.554	0.007	5	-0.003	-0.25	9 3 6	17734.243 n	0.001	2	0.007	-0.24
5 3 3	17246.451	0.006	3	-0.012	-0.23	9 4 5	17789.389 n	0.002	2	0.005	-0.27
5 3 2	17248.521	0.005	4	0.003	-0.22	9 5 5	17874.758		1	-0.006	-0.23
5 4 2	17321.009	0.003	2	0.003	-0.20	9 5 4	17875.474	0.014	2	0.004	-0.19
5 4 1	17321.083	0.006	3	0.001	-0.20	9 6 4	17987.194 n	0.006	2	0.016	-0.12
5 5 1	17415.788	0.003	3	0.005	-0.16	9 6 3	17987.199 n	0.011	2	-0.010	-0.18
5 5 0	17415.788	0.003	3	0.005	-0.17	10 0 10*	17640.638 n	0.001	2	0.152	-0.46
6 0 6	17207.933	0.001	3	-0.001	-0.25	10 1 10	17640.481 n	0.001	3	0.014	-0.48
6 1 6	17208.499	0.003	4	-0.001	-0.26	10 1 9	17751.320 n	0.002	2	-0.024	-0.27
6 1 5	17265.898	0.004	5	0.001	-0.25	10 2 9	17752.005 n	0.009	3	-0.013	-0.27
6 2 5	17274.881		1	-0.001	-0.24	10 2 8	17838.941 c	0.006	3	-0.007	-0.45
6 2 4	17302.041	0.004	3	-0.005	-0.26	10 3 8*	17847.333 c	0.008	2	0.049	-0.43
6 3 4	17338.055	0.006	3	-0.011	-0.24	10 3 7*	17897.061	0.003	2	-0.054	-0.35
6 3 3	17343.658	0.002	2	-0.001	-0.24	10 5 6	18028.399	0.006	2	0.011	-0.39
6 4 3	17412.935	0.002	4	-0.001	-0.20	11 0 11	17778.257 c	0.002	2	0.001	-0.53
6 4 2	17413.298	0.007	4	-0.002	-0.20	11 1 11*	17778.304 c		1	0.040	-0.57
6 5 2	17507.250	0.002	3	-0.002	-0.17	11 1 10	17901.399 n		1	-0.021	-0.27
6 5 1	17507.251	0.003	3	-0.009	-0.17	11 2 10	17901.751 n	0.004	2	0.016	-0.28
6 6 1	17621.655	0.003	2	0.004	-0.12	11 2 9	18003.034 n		1	0.018	-0.50
6 6 0	17621.655	0.003	2	0.004	-0.12	11 3 9*	18007.888 n		1	0.165	-0.47
7 0 7	17298.279	0.004	4	0.001	-0.26	11 4 8	18101.707 n		1	-0.003	-0.41
7 1 7	17298.532	0.005	4	0.002	-0.25	11 4 7	18128.070 n		1	-0.008	-0.50
7 1 6	17370.163	0.003	4	-0.002	-0.25	12 0 12	17927.879 n	0.001	2	0.001	-0.55
7 2 6	17375.407	0.005	3	0.002	-0.24	12 1 12	17927.879 n	0.001	2	0.004	-0.52
7 2 5	17416.132 n	0.004	3	-0.005	-0.25	12 1 11	18063.168 n	0.001	2	0.001	-0.44
7 3 5	17444.454 n	0.004	2	0.007	-0.23						
								(104)			
						9 6 4	17615.299		1		0.24

Note. Asterisks denote the energy levels excluded from the fitting. n denotes newly derived energy levels compared to Ref. (*5*). c denotes corrected levels compared to Ref. (*5*). σ denotes the experimental uncertainty of the level in cm^{-1}. N is the number of lines sharing the same upper level. Δ is the difference between the experimental energy levels and the predictions of Ref. (*12*).

TABLE 3
Spectroscopic Constants of the (0 0 5) Vibrational State of HDO (in cm^{-1})

E_v	16920.02401(220)
A	18.514220(540)
B	9.044449(120)
C	6.0126750(100)
Δ_k	$8.3560(340) \times 10^{-3}$
Δ_j	$4.31336(360) \times 10^{-4}$
δ_k	$1.32111(370) \times 10^{-3}$
δ_j	$1.57756(360) \times 10^{-4}$
H_k	$2.0579(630) \times 10^{-5}$
H_{jk}	$4.683(220) \times 10^{-7}$

TABLE 4
Transition Moment Parameters (in D) for the (0 0 5) Vibrational State of HDO

N^a	*a*-type	*b*-type
1	$1.0352(110) \times 10^{-4}$	$2.3391(430) \times 10^{-5}$
2	$4.378(880) \times 10^{-8}$	0
4	0	$-1.0701(920) \times 10^{-6}$
5	$8.35(160) \times 10^{-8}$	$1.2834(610) \times 10^{-6}$
6	$5.763(960) \times 10^{-7}$	0
Number of transitions	187	40
δ^b	13%	

[a] Numbering of the parameters (from 1 to 8) as defined in Ref. (*16*).
[b] $\delta = |I_{obs} - I_{calc}|/I_{obs}$ in percent.

5) and the sum of these intensities is close to the unperturbed *a*-type intensity revealing an important intensity transfer from *a*- to *b*-type transitions. This intensity transfer frequently takes place between different vibrational bands. It was, however, observed within a single band (*2*), namely the $\nu_2 + 4\nu_3$ band of HDO, and explained as a result of the simultaneous occurrence of strong anharmonic and rovibrational interactions in the molecules of C_s symmetry. Finally, as shown in Table 5, the predicted intensity transfer from the considered $5\nu_3$ transitions to the (unobserved) line partner of the $\nu_1 + 4\nu_3$ band is considerably less pronounced than that between the *a*- and *b*-type transitions of the $5\nu_3$ band itself.

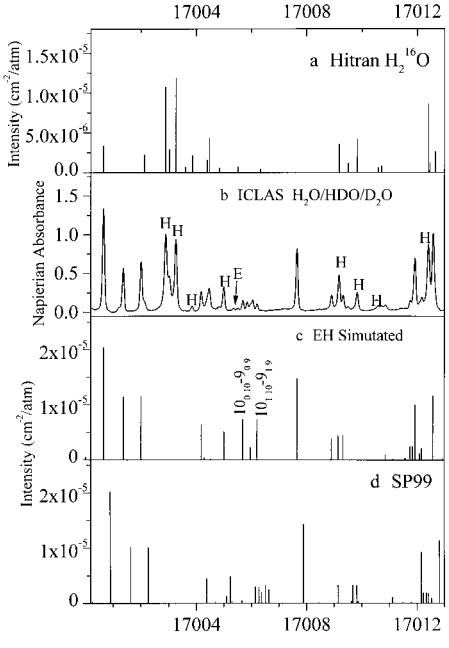

FIG. 2. Comparison of the HDO absorption spectrum in the 17 000.2–17 013 cm^{-1} spectral region. (a) Stick spectrum of $H_2{}^{16}O$ as given in HITRAN (*10*). (b) ICLAS spectrum of a 1:1 mixture of D_2O and H_2O recorded with an equivalent path length of 12 km and a total vapor pressure of about 13 Torr. Lines of H_2O are marked by H; the other lines are due to HDO. The line at 17 005.352 cm^{-1}, marked by E, is an extra line assigned to the [9 6 4]–[8 2 7] transition of the $\nu_1 + 4\nu_3$ band (see text). (c) Synthetic spectrum obtained from the effective Hamiltonian (EH) approach. (d) *Ab initio* spectrum predicted by Ref. (*12*). Note the resonance intensity transfer within the clump of lines near 17 006 cm^{-1} (see also the text).

The orientation of the transition dipole-moment vector, derived from the ratio of fractional *a*- and *b*-type transition intensities, has proven to be quite sensitive to the quality of the dipole-moment surface of the HDO molecule (*4*). It is then interesting to compare the intensity ratio obtained for the $5\nu_3$ band with the values estimated for the lower $n\nu_3$ bands as well as with the predictions of Refs. (*12, 15*) (see Table 6). Using the same procedure as described in Ref. (*4*), the angle, $\theta_{\nu'-\nu''}$, between the transition moment in a given vibrational state and the OH bond can be estimated from the ratio of the total *a*- and *b*-type intensities of the corresponding band. For the $5\nu_3$ band, $I_a/I_b = 20$ leads to $\theta_{\nu'-\nu''} = 46.4°$, which is consistent with an increase from 26.4° up to 36.7° observed between $n = 1$ and $n = 4$. The *a*-type character increasing with the OH vibrational excitation is a consequence of the increased tilt of the transition dipole-moment vector away from the OH bond (*4*). The comparison provided in Table 6 shows that this variation is quantitatively predicted by the dipole moment surface calculated by Partridge and Schwenke (*12, 15*). Note that the $I_a/I_b = 1.4$ intensity ratio (*26*) adopted in Ref. (*4*) for the ν_3 fundamental differs significantly from the more recent results of Ref. (*17*), which agree perfectly with the predictions of Ref. (*15*).

Assuming that the HOD angle is fixed at 104.5° (*4, 15*), the angle, $\theta_{\nu'-\nu''}$, between the transition moment in a given vibrational state and the OD bond is given by

$$\theta_{\nu'-\nu''} = \theta_a + 16.5°, \qquad [2]$$

where $I_a/I_b = 1/tg^2(\theta_a)$. Using this expression and the I_a/I_b intensity ratio provided either by the experiment or by the predictions of Refs. (*12, 15*), the $\theta_{\nu'-\nu''}$ angle relative to the OD bond is calculated for the $n\nu_1$ sequence (see Table 6). The $5\nu_1$

TABLE 5
Resonance Intensity Transfer from *a*- to *b*-Type Transitions Within the $5\nu_3$ Band of HDO

Wavenumber (cm^{-1}) Pred. (*12*)	Observed	State	JK_aK_c	JK_aK_c	Intensity (cm^{-2}/atm) Obs.	*EH*	Pred. (*12*)
17006.635	17006.209	0 0 5	10 0 10	9 0 9	2.7E-06	7.3E-06	2.4E-06
17006.273	17005.848	0 0 5	10 0 10	9 1 9	3.1E-06	2.3E-09	2.9E-06
17006.508	17006.052	0 0 5	10 1 10	9 0 9	3.5E-06	2.3E-09	3.3E-06
17006.145	17005.692	0 0 5	10 1 10	9 1 9	3.5E-06	7.3E-06	3.0E-06
17005.656	-	1 0 4	10 5 6	9 0 9	-	-	5.0E-07
17005.295	-	1 0 4	10 5 6	9 1 9	-	-	3.7E-07
				Total	12.8E-06	14.6E-06	12.5E-06

and $6\nu_1$ bands are very weak bands with a strong hybrid character (*2, 24, 25*); the value of 1 adopted for the experimental I_a/I_b intensity ratio of these two bands is a very rough estimation. The results gathered in Table 6 show that the evolution of the hybrid character of the OD and OH stretching overtone bands is opposite: the $n\nu_1$ bands have a strong *a*-type character for small *n* values which evolve toward a pronounced hybrid character for $n = 5$ and 6, while the low OH stretching overtones are hybrid bands and become *a*-type bands as *n* increases. On the other hand, the angle between the transition-moment vector and the stretching bond shows a very similar behavior as a consequence of the independence upon deuteration of both the potential energy surface and the dipole-moment surface. Once more, the predictions of Refs. (*12, 15*) agree fairly well with the available experimental data. As previously analyzed in Ref. (*3*), the new predictions of Ref. (*12*) based on an improved dipole-moment surface appear to be significantly more accurate at high vibrational excitation. For instance, the $6\nu_1$ band is predicted with a pronounced hybrid character (*12*) in agreement with the experiment (*2*), while a dominating *a*-type character was previously predicted for this band (*15*).

4. CONCLUSION

The high sensitivity of the ICLAS technique has allowed an improved analysis of the rotational energy pattern of the (0 0 5) state of HDO. The extended set of energy levels, mostly unaffected by interaction with the other nearby states, could be modeled, at the experimental accuracy level, in the effective Hamiltonian approach. From the fractional *a*- or *b*-type intensities, the tilt of the transition moment vector away from the OH bond has been analyzed and compared to recent predictions of Schwenke and Partridge (*12, 15*). A similar discussion relative to the OD stretching overtones has shown that, in spite of an opposite dependence of the hybrid character upon stretching excitation, the tilt of the transition moment vector compared to the OD bond is similar to that observed in the OH

TABLE 6
Experimental and Theoretical (*12*) Angles of the Transition Dipole Moment Vector Relative to the OH and OD Bonds for the $n\nu_3$ and $n\nu_1$ Bands of HDO

	ν_0 (cm^{-1})	I_a/I_b Obs.	Pred.[f]	$\theta_{v'-v''}$(deg.) Obs.	Pred.
ν_3	3707.467[a]	2.4[a]	2.4	26.4	26.2
$2\ \nu_3$	7250.519[b]	1.9[g]	1.8	23.0	22.3
$3\ \nu_3$	10631.636[c]	2.7[c]	3.5	27.7	30.9
$4\ \nu_3$	13853.631[d]	5.9[d]	7.7	36.7	36.6
$5\ \nu_3$	16920.028[e]	20.0[e]	23.7	46.4	47.4
$6\ \nu_3$	19863.68[f]		82.3		52.7
ν_1	2723.680[h]	47.0[i]	76.9	24.8	23.0
$2\ \nu_1$	5363.824[j]	73.1[k]	77.5	23.2	23.0
$3\ \nu_1$	7918.13[f]		13.7		31.6
$4\ \nu_1$	10378.64[f]		5.8		39.0
$5\ \nu_1$	12767.126[l]	≈1[l]	2.1	≈62	51.1
$6\ \nu_1$	15065.712[m]	≈1[m]	1.5	≈62	55.7

[a] Ref. (*17*).
[b] Ref. (*18*).
[c] Ref. (*4*).
[d] Ref. (*1*).
[e] This work, calculated value from the transition moment parameters of Table 4.
[f] Predicted values of Ref. (*12*).
[g] Ref. (*19*).
[h] Ref. (*20*).
[i] Ref. (*21*).
[j] Ref. (*22*).
[k] Ref. (*23*).
[l] Refs. (*24, 25*).
[m] Ref. (*2*).

stretching series. The present study confirms the quality of the energy levels predictions of Refs. (*12*, *15*) and the significant improvement of the line intensity predictions of Ref. (*12*) compared to Ref. (*15*). It also would be interesting to compare these results with those obtained with the recently published ground state PES of water by Kain *et al.* (*27*). In this latter study a pure *ab initio* PES (*15*, *28*) was improved by including correction to the bending potential that resulted in a significant improvement of the predicted vibrational band origins.

ACKNOWLEDGMENTS

O. Naumenko thanks the University Joseph Fourier of Grenoble for the Visiting Professorship, during which this work was carried out, and acknowledges as well the financial support from the Russian Foundation for Basic Researches, Grant 99-03-33210. E. Bertseva acknowledges the financial support from the Rhône-Alpes region in the frame of the TEMPRA exchange program. The expert help of G. Weirauch during the recording of the spectra is also acknowledged. We are grateful to D. Schwenke and H. Partridge for access to HDO calculations and to J. Liévin for correspondence.

REFERENCES

1. O. Naumenko, E. Bertseva, and A. Campargue, *J. Mol. Spectrosc.* **197,** 122–132 (1999).
2. O. Naumenko and A. Campargue, *J. Mol. Spectrosc.* **199,** 59–72 (2000).
3. O. Naumenko, E. Bertseva, A. Campargue, and D. Schwenke, *J. Mol. Spectrosc.* **201,** 297–309 (2000).
4. R. Fair, O. Votava, and D. J. Nesbitt, *J. Chem. Phys.* **108,** 72–80 (1998).
5. A. D. Bykov, V. A. Kapitanov, O. V. Naumenko, T. M. Petrova, V. I. Serdukov, and L. N. Sinitsa, *J. Mol. Spectrosc.* **153,** 197–207 (1992).
6. (a) O. Votava, J. R. Fair, D. F. Plusquellic, E. Riedle, and D. J. Nesbitt, *J. Chem. Phys.* **107,** 8854–8865 (1997); (b) R. L. Vander Wal, J. L. Scott, F. F. Crim, K. Weide, and R. Schinke, *J. Chem. Phys.* **94,** 3548–3555 (1991); (c) A. Sinha, M. C. Hsiao, and F. F. Crim, *J. Chem. Phys.* **94,** 4928–4935 (1991).
7. M. Brouard and S. R. Langford, *J. Chem. Phys.* **106,** 6354–6364 (1997).
8. A. Campargue, M. Chenevier, and F. Stoeckel, *Spectrochim. Acta Rev.* **13,** 69–88 (1990).
9. M. Herman, J. Liévin, J. Van der Auwera, and A. Campargue, *Adv. Chem. Phys.* **108,** 1–431 (1999).
10. L. S. Rothman, C. P. Rinsland, A. Goldman, S. T. Massie, D. P. Edwards, J.-M. Flaud, A. Perrin, C. Camy-Peyret, V. Dana, J.-Y. Mandin, J. Schroeder, A. McCann, R. R. Gamache, R. B. Wattson, K. Yoshino, K. V. Chance, K. W. Jucks, L. R. Brown, V. Nemtchinov, and P. Varanasi, *J. Quant. Spectrosc. Radiat. Transfer* **60,** 665–710 (1998).
11. S. Gerstenkorn and P. Luc, "Atlas du Spectre d'Absorption de la Molécule d'Iode," Edition du CNRS, Paris, 1978.
12. D. Schwenke and H. Partridge, *J. Chem. Phys.*, in press.
13. R. Toth, *J. Mol. Spectrosc.* **162,** 20–40 (1993).
14. A. D. Bykov, V. S. Makarov, N. I. Moskalenko, O. V. Naumenko, O. N. Ulenikov, and O. V. Zotov, *J. Mol. Spectrosc.* **123,** 126–134 (1987).
15. H. Partridge and D. Schwenke, *J. Chem. Phys.* **106,** 4618–4639 (1997).
16. C. Camy-Peyret and J.-M. Flaud, *in* "Molecular Spectroscopy: Modern Research" (K. Narahari Rao, Ed.), Vol. III, pp. 69–109, Academic Press, New York, 1985.
17. R. A. Toth and J. W. Brault, *Appl. Opt.* **22,** 908–926 (1983).
18. R. Toth, *J. Mol. Spectrosc.* **186,** 66–89 (1997).
19. A. D. Bykov, O. V. Naumenko, T. M. Petrova, and L. N. Sinitsa, *Atmos. Oceanic Opt.* **11,** 1281–1289 (1998).
20. N. Papineau, C. Camy-Peyret, J.-M. Flaud, and G. Guelachvili, *J. Mol. Spectrosc.* **92,** 451–468 (1982).
21. A. Perrin, J.-M. Flaud, and C. Camy-Peyret, *J. Mol. Spectrosc.* **112,** 156–162 (1985).
22. R. Toth, *J. Mol. Spectrosc.* **186,** 276–292 (1997).
23. A. D. Bykov, O. V. Naumenko, T. M. Petrova, and L. N. Sinitsa, unpublished results.
24. S. Hu, H. Lin, S. He, J. Cheng, and Q. Zhu, *Phys. Chem. Chem. Phys.* **1,** 3727–3730 (1999).
25. V. Lazarev, T. Petrova, L. Sinitsa, Q.-S. Zhu, J.-X. Han, and L. Y. Hao, *Atmos. Oceanic Opt.* **11,** 809–812 (1998).
26. W. S. Benedict, N. Gailar, and E. K. Plyler, *J. Chem. Phys.* **24,** 1139–1165 (1956).
27. J. S. Kain, O. L. Polyansky, and J. Tennyson, *Chem. Phys. Lett.* **317,** 365–371 (2000).
28. O. L. Polyansky, J. Tennyson, and N. F. Zobov, *Spectrochem. Acta, Part A* **55,** 659 (1999).